Complex Branching Patterns in a Newly Recognized Species of *Compsocradus* Berry et Stein (Iridopteridales) from the Middle Devonian of North Xinjiang, China
Author(s): Qiang Fu, Yi Wang, Christopher M. Berry, and Hong-He Xu
Source: *International Journal of Plant Sciences*, Vol. 172, No. 5 (June 2011), pp. 707-724
Published by: The University of Chicago Press
Stable URL: http://www.jstor.org/stable/10.1086/659453
Accessed: 21/02/2014 08:49

Int. J. Plant Sci. 172(5):707–724. 2011.

1058-5893/2011/17205-0009$15.00 DOI: 10.1086/659453

COMPLEX BRANCHING PATTERNS IN A NEWLY RECOGNIZED SPECIES OF *COMPSOCRADUS* BERRY ET STEIN (IRIDOPTERIDALES) FROM THE MIDDLE DEVONIAN OF NORTH XINJIANG, CHINA

Qiang Fu,* Yi Wang,[1],* Christopher M. Berry,† and Hong-He Xu*,†

*State Key Laboratory of Palaeobiology and Stratigraphy, Nanjing Institute of Geology and Palaeontology, Chinese Academy of Sciences, 210008 Nanjing, People's Republic of China; and †School of Earth and Ocean Sciences, Cardiff University, Park Place, Cardiff CF10 3YE, United Kingdom

Specimens, including the largest known axes, of an iridopteridalean plant of late Middle Devonian age are described from northern Xinjiang, China. The plant consists of three orders branching and dichotomous appendages. The first-order axis probably represents the stem. Lateral organs (lower-order branches and appendages) are attached along the primary axis in up to 10 ranks. The insertion pattern can be broken down into cycles in which one lateral is inserted in each rank, and each cycle is divided into two loose whorls; in one loose whorl, laterals occur in about half of the ranks, some adjacent, and in the other loose whorl, laterals occur in the other ranks. These ranks are believed to map the position of xylem ribs of the vascular system, which has not been preserved. The appendages are isodichotomously divided up to five times. Pairs of recurved sporangia terminate the fertile appendages. A collection of small axes (second and third order) of this plant from the same locality, lacking the distinctive branching patterns displayed in our first order axes, was recently given the name *Ramophyton givetianum* by D. M. Wang. Our enlarged concept of the plant includes several morphological similarities to *Compsocradus laevigatus* Berry et Stein from Venezuela, particularly relating to the branching pattern. The Xinjiang plant is therefore reassigned to *Compsocradus givetianus* (Wang DM) Fu, Wang Y, Berry et Xu comb. nov. It further increases knowledge of branching patterns amongst Iridopteridales, important for evaluating relationships to other plant groups.

Keywords: Iridopteridales, plant fossils, morphology, apical development.

Introduction

Iridopteridales was erected by Stein (1982) on the basis of anatomical characters of permineralized axes. Middle and Late Devonian iridopteridaleans are characterized by a deeply ribbed mesarch actinostele with two or three centrally united primary xylem segments (Berry and Stein 2000). These ribs may divide to form up to 20 radial outer ribs. Branching patterns are essentially whorled, with traces to lateral branches or dichotomous appendages emitted from single protoxylem poles permanently located near the extremities of each rib. Middle Devonian taxa currently included in this group are as follows: based on anatomy, *Iridopteris* Arnold 1940, *Arachnoxylon* Read 1938, *Asteropteris* Dawson 1881, and *Rotoxylon* Cordi et Stein 2005; based on anatomy and morphology, *Ibyka amphikoma* Skog et Banks 1973, *Compsocradus* Berry et Stein 2000, and *Metacladophyton* Wang et Geng 1997 (see Berry and Stein 2000; Wang and Lin 2007); and based on compressions alone, *Anapaulia* Berry et Edwards 1996 and *Ibyka vogtii* (Høeg) Berry (see Berry 2005). These latter compression fossils have lateral branches and dichotomous appendages inserted on the largest axis in a pattern directly corresponding to the branching as characterized anatomically in, for example, *Arachnoxylon* and have morphology very similar to *I. amphikoma*. Branches and appendages are inserted in whorls, with one branch or appendage positioned in each rank corresponding to the number of ribs in the stele, an apparently unique organotaxis for Middle Devonian plants. The plants of this group are potentially intermediate between Early Devonian basal euphyllophytes (Kenrick and Crane 1997) and the more complex Late Devonian/Mississippian major groups, for example, sphenopsids and ferns (Arnold 1940; Skog and Banks 1973; Stein et al. 1984; Berry and Stein 2000).

In terms of paleogeographical distribution, most known Middle Devonian iridopteridaleans come from Laurentia (North America, Svalbard). However, Berry and Fairon-Demaret (2001) suspect a much wider distribution of this group.

Compsocradus laevigatus Berry et Stein (2000), from the Middle or earliest Late Devonian of western Venezuela, is one of the most completely known iridopteridaleans, with both external morphology and internal anatomy partly understood. Morphologically, *C. laevigatus* is characterized by a pseudomonopodial branching system, with two known axis orders; the surfaces of axes lack spines and have longitudinal folds and inverted U-shaped scars marking the insertion of laterals; second-order axes are narrower and shorter, inserted acutely; appendages consist of narrow axes branched predominantly isotomously, successive dichotomies being approximately perpendicular; fertile appendages terminate in erect paired sporangia, and sterile appendages

---

[1] Author for correspondence; e-mail: yiwang@nigpas.ac.cn.

Manuscript received July 2010; revised manuscript received December 2010.

terminate with oppositely recurved tips. It has a typically iridopteridalean stele resembling in form the anatomically preserved *Arachnoxylon*. Until the description of *Compsocradus*, all iridopteridaleans were believed to have a branching pattern with whorls of emitted branches and appendages, one emitted for each rib at a whorl. In *Compsocradus*, the branching was suggested to be whorled but with laterals emitted from every other xylem rib at a whorl, with the alternate ribs involved in alternate whorls. Cordi and Stein (2005) described a short permineralized axis, *Rotoxylon dawsonii* (Dawson) Cordi et Stein, in which the pattern of trace emission—and therefore potentially the insertion of lateral branches and appendages—may be even more complex.

Wang et al. (2004) reported the first discoveries of a diverse assemblage of plant fossils from a new locality in Xinjiang, northwest China, known informally to us as 251 Hill, including the first mention of the presence of *Compsocradus* sp. outside Venezuela. The locality yielded enough material for (so far) two complete PhD dissertations. Xu (2006) reported numerous lycopsid species, including *Haskinsia sagittata* and *Haskinsia hastata* (Xu et al. 2008). Fu (2006) described the nonlycopsid flora, including substantial material of a new species of *Compsocradus*. Preparation, description, and analysis of this material, carried out in Nanjing and Cardiff, concentrated on the understanding of the complex branching patterns found on the largest axes of up to three orders of branching in organic connection. The recognized patterns of branching were validated by new observations on the type collection of *C. laevigatus* from Venezuela, reported at the end of this article.

During our elaboration of these materials for publication, Wang (2008) published an account of the second and third order of branching of the plant from the same locality under the name *Ramophyton givetianum* Wang. In this article, we provide a comprehensive account of the branching patterns of the plant and reassign it to *Compsocradus givetianus* (Wang DM) Fu, Wang Y, Berry et Xu comb. nov.

Material and Methods

All fossils described here were found in the Hujiersite Formation (Xiao et al. 1992). They were collected from a 1-m-thick lens of gray-yellow mudstones and quartzose sandstone within a prominent conglomerate layer on the south slope of a small hill (251 Hill), ~20 km north of Hostuleke (Hoxtolgay) town, Hobuksar Menggol Autonomous County, North Xinjiang, China (fig. 1; 86°01′06.3″E, 46°36′54.7″N [WGS84 datum]). Of the 12 m or so of sediments exposed here, there are mostly thin beds of gray and green mudstones with two rooted horizons, granule and pebble conglomerates with erosive bases, a thick sandstone horizon, and a coal horizon ~20 cm thick at the top. We therefore interpret these beds as terrestrial alluvial floodplain and channel environments.

On the basis of spores recovered from the type section of the Hujiersite Formation, ~80 km to the northeast of 251 Hill (Lu 1997), and the study of conchostracans by Liu (1990), the age of the Hujiersite Formation is regarded as late Middle Devonian (Givetian; also see Cai and Wang 1995; Lu 1997; Cai 2000; Wang et al. 2004). Dating of the 251 Hill locality directly based on spores is presently being attempted (J. E. A. Marshall, personal communication), suggesting a slightly older age is also possible. Plants from the

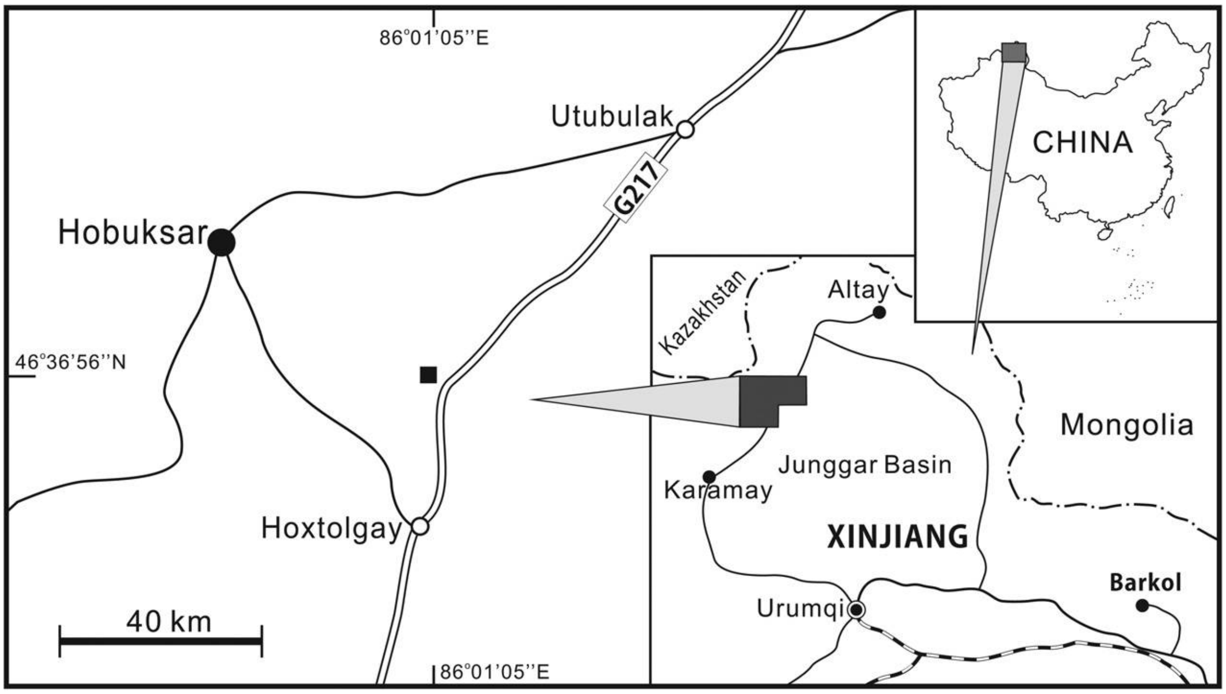

Fig. 1 Map of the 251 Hill fossil locality (black square), 20 km north of Hostuleke town, Hobuksar Menggol Autonomous County, North Xinjiang, China.

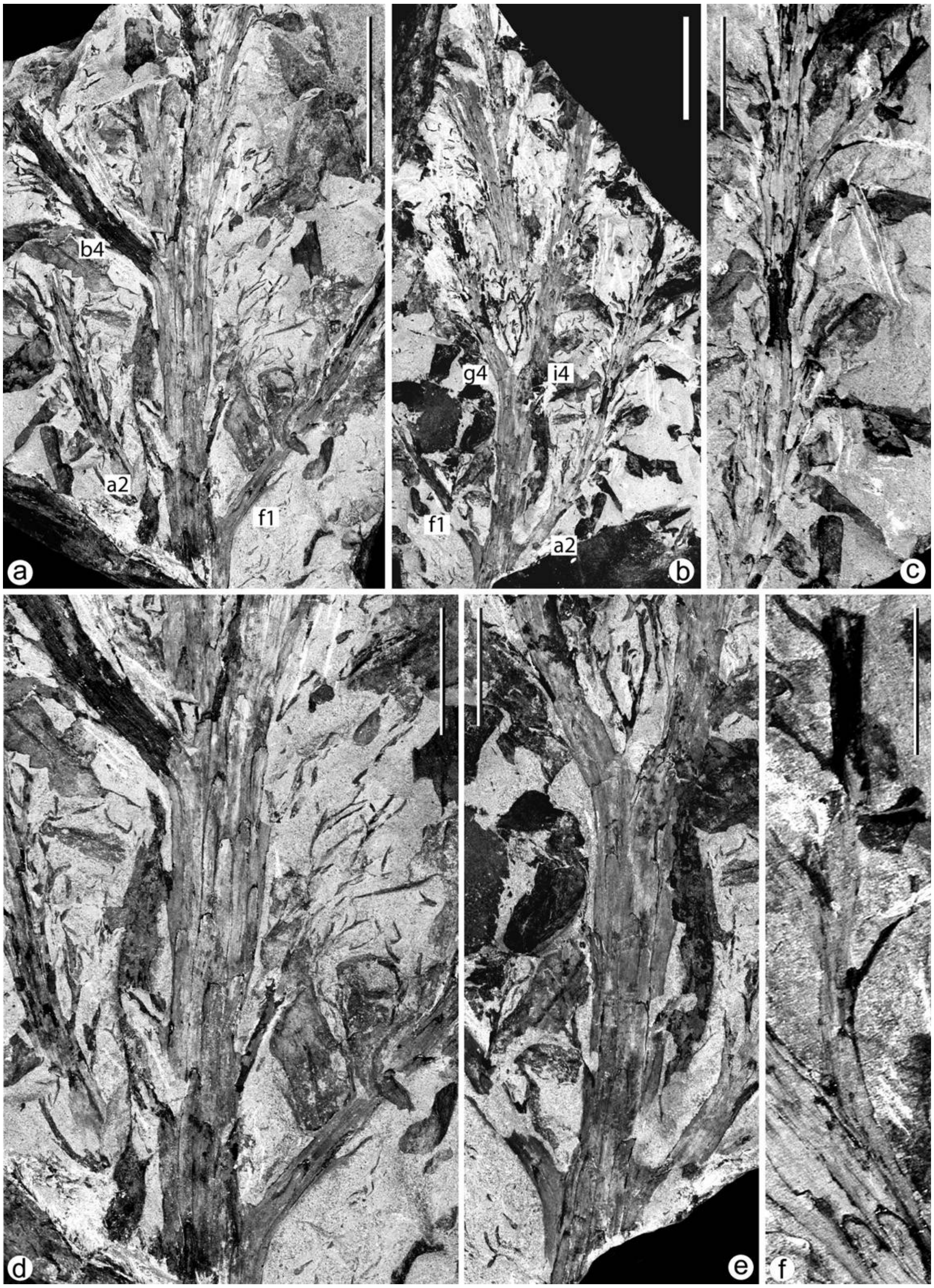

Fig. 2 *Compsocradus givetianus* (Wang DM) Fu, Wang Y, Berry et Xu comb. nov. from Xinjiang. *a*, *b*, Part and counterpart, first-order axis with second-order axis and appendages (see fig. 3). Specimen PB 20322a&b. Scale bar = 20 mm. *c*, Second-order axis with third-order axis and appendages, from the right second-order axis in *b*. Scale bar = 10 mm. *d*, *e*, Part and counterpart, first-order axis with U-shaped appendage bases, from *a* and *b* (see fig. 4). Scale bar = 10 mm. *f*, Third-order axis with appendages, from *c*. Scale bar = 5 mm.

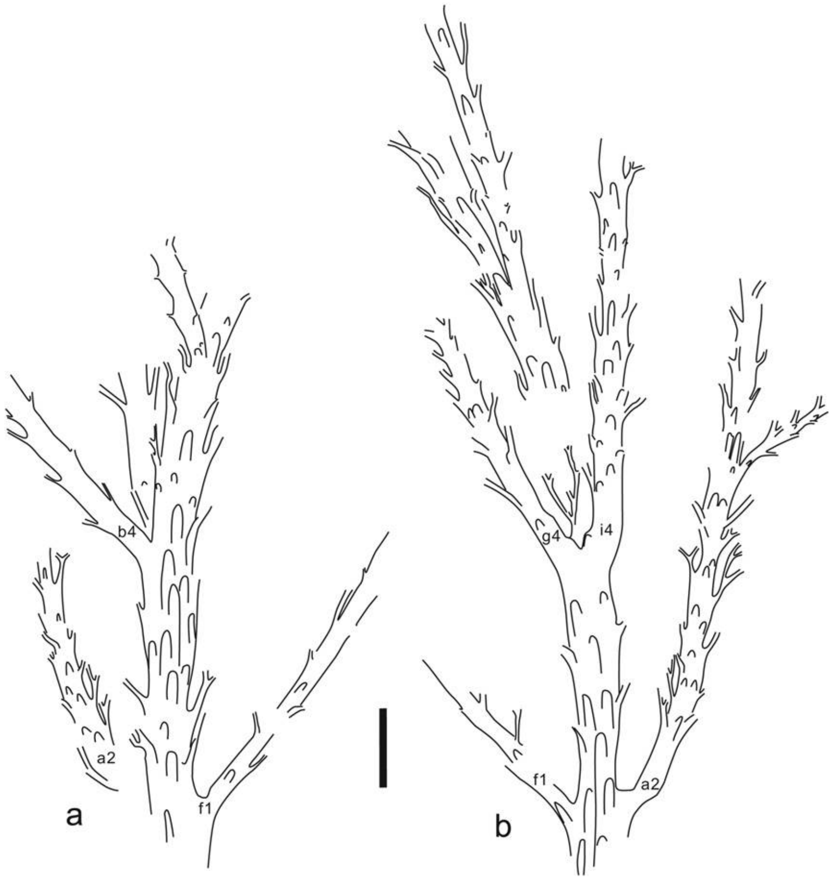

Fig. 3 *Compsocradus givetianus* (Wang DM) Fu, Wang Y, Berry et Xu comb. nov. from Xinjiang. Line drawing of first- to third-order axes of part and counterpart specimen PB 20322a&b. *a*, Part after dégagement (see fig. 2*a*). *b*, Counterpart after dégagement (see fig. 2*b*). Scale bar = 10 mm.

locality include the lycopsids *Lepidodendropsis theodori* (Zal.) Jongmans, *Lepidodendropsis kazachstanica* Senkevitsch, *Haskinsia sagittata* Edwards et Benedetto, *Leclercqia* sp., *Colpodexylon* sp., the zosterophyll *Serrulacaulis* sp., the "trimerophyte" *Tsaia conica* Wang, Xu, Fu et Tang (Wang et al. 2004; Fu 2006; Xu 2006), and several as yet unknown taxa. Compared with the paleofloras of New York State and Venezuela (Banks 1980; Berry and Edwards 1996; Berry and Stein 2000), particularly the presence of *Haskinsia*, *Colpodexylon*, and *Serrulacaulis*, this flora also suggests a late Middle Devonian (Givetian) age (Edwards et al. 2000). Differences between the palynofloras and macrofossil assemblages at 251 Hill and the type Hujiersite section have also become apparent. Therefore, we presently assign only the 251 Hill specimens a Middle Devonian age.

The fossils are preserved predominantly as impressions and coalified compressions. Three-dimensional architecture was revealed by dégagement (Leclercq 1960; Fairon-Demaret et al. 1999). Macrophotographs were taken using a Nikon D-100 camera, 100-mm macro lens, and crossed polarized illumination. Microphotographs were taken using a Leica MZ-12 stereomicroscope with annular ring illumination.

Figured specimens are housed at the Nanjing Institute of Geology and Palaeontology, Chinese Academy of Science, prefix PB. The type material and other specimens described by D. M. Wang are located in the Department of Geology, Peking University, Beijing. Venezuelan specimens are retained in the National Museum and Gallery, Cardiff, Wales, prefix NMW.

Branching Patterns: Methodology and Terminology

Central to the description of the fossils described here is accurately recording the pattern of branching. Branching patterns in Devonian land plant organs with a central major axis are generally characterized as helical (spiral) or whorled or variations on these. The branching pattern and shape of the stele is established by the behavior of the shoot apical meristem and production of primordia (Wight 1987; Stein 1993). According to this proposed relationship, in protostelic plants the positions of the laterals are effectively related to the position of primary xylem ribs. Protoxylem and primary xylem of vascular traces diverge from the ribs and travel out obliquely through the cortex until they emerge as the organ at the surface. Typical helical insertion in basal euphyllophytes is recognized by lateral departures spaced at regular divergence angles (i.e., angles in the transverse plane between successive elements of a single ontogenetic helix). With a single ontogenetic helix, only one lateral is positioned at each node on the axis. In cases of more than one ontogenetic helix, including whorled branching, multiple laterals are emitted at the same level

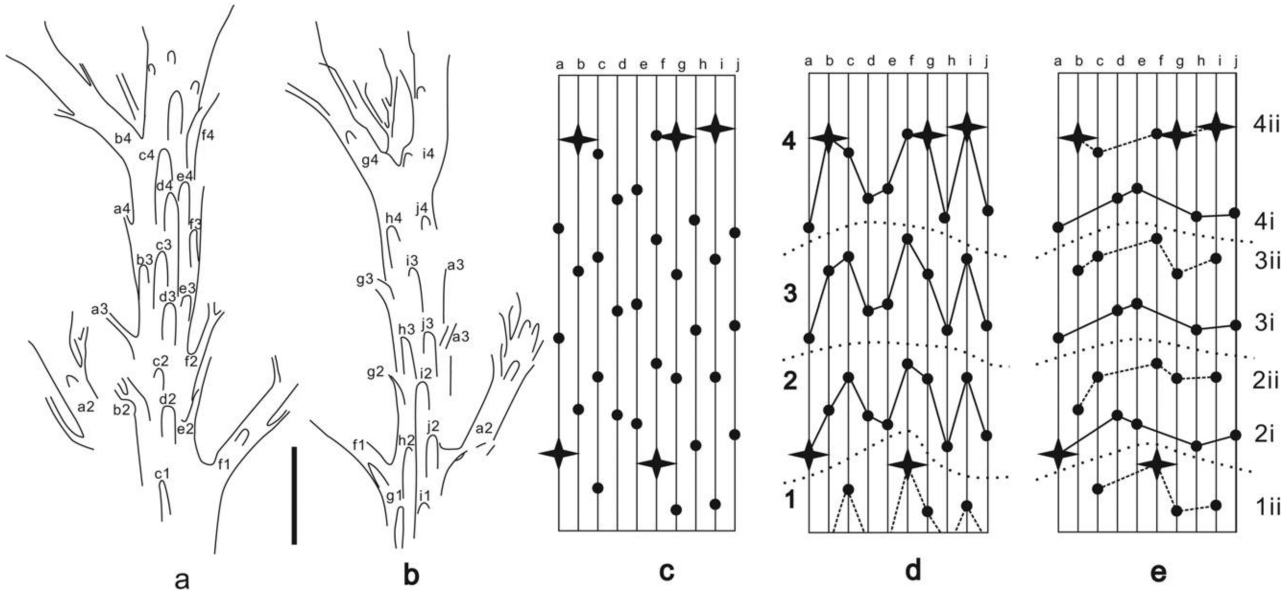

Fig. 4 *Compsocradus givetianus* (Wang DM) Fu, Wang Y, Berry et Xu comb. nov. from Xinjiang. Line drawing of the first-order axis after dégagement, specimen PB 20322a&b. *a*, *b*, Part and counterpart (see fig. 2*d*, 2*e*). *c–e*, Diagrammatic representation of the insertion of appendages and branches organs spread around the complete axis. Circles = appendages; stars = second-order branches. *c*, All bases. *d*, Bases divided into four cycles (1–4). *e*, Cycles divided into two loose whorls (i, ii). Scale bar = 10 mm.

(node) on the axis surface. In some instances, as suspected here, successive whorls show regular offset in the pattern of insertion, with or without pronounced internodes.

We first established from each compression fossil, part and counterpart, the longitudinal (i.e., along-axis) position of insertion of each lateral (fig. 4*a*–4*c*). In addition, longitudinal folds in the axis surfaces strongly suggest the occurrence of longitudinal ranks (orthostichies) of insertion, presumably representing the internal position of xylem ribs, which were given letters (e.g., *a*, *b*, *c*). We noticed early on that, working longitudinally along the axis, most often one base occurred in each identified rank before any rank gave off a second lateral. This led us to first present our branch base data in a graphical style, which emphasizes the rank of branch bases within every cycle of bases (i.e., a set of longitudinally adjacent laterals, one from each of the ranks, *a*–*x*), where the symbols representing lateral bases within the cycles were linked by lines (fig. 4*d*). Linking branch bases from laterally adjacent ranks (fig. 4*d*) suggest a regular phyllotaxis consisting of presumptive whorls with large uncertainty of longitudinal position (suggested by zigzag lines). Alternatively, linking branch bases in presumptive whorls that involve more or less regular angular offset (fig. 4*e*) show apparently much less uncertainty (and correspondingly less zigzagged lines).

Our results show that phyllotaxis in this plant is not random but is rather organized. Options for interpreting this phyllotactic pattern include (1) a single ontogenetic helix, (2) multiple ontogenetic helices, (3) whorled phyllotaxis with a branch base in each longitudinal rank (orthostichy) per whorl, and (4) whorled phyllotaxis with only some branch bases present in each whorl and whorls showing more or less regular angular offset. Our graphical results suggest the presence of whorls, albeit not strict whorls with laterals inserted at the same level. Lacking anatomical understanding, we might rather describe them as loose whorls. Less variance in longitudinal position within whorls supports option 4 over option 3.

Systematic Paleobotany

Order—Iridopteridales Stein 1982

*Genus—*Compsocradus *Berry et Stein 2000 emend.*

Emended generic diagnosis. Plants pseudomonopodial. At least three orders of axes known, with external surfaces lacking emergences. Lower orders of axes bear both higher-order axes and dichotomous appendages. Ultimate appendages consisting of narrow axes branched predominantly isotomously, successive dichotomies being approximately perpendicular; fertile appendages terminate in erect or recurved paired sporangia; sterile ultimate appendages terminate with oppositely recurved tips. Both ultimate appendages and second-order axes are arranged in loose whorls on first-order axes, with attachments alternating in successive whorls; insertion patterns become less clear in higher-order axes. Protostele ribbed, mesarch, with six primary xylem ribs; traces arising from every other rib at each whorl, successive whorls alternating; a similar pattern inferred from compression material, some branches and appendages in whorls may occur in neighboring ranks, up to 10 ranks on the largest axes. Protoxylem strands located permanently peripherally, one in each primary xylem rib; tracheids with uniseriate circular to oval bordered pits.

Type species. *Compsocradus laevigatus* Berry et Stein 2000. *Compsocradus givetianus* (Wang DM) Fu, Wang Y, Berry et Xu comb. nov. (figs. 2–15).

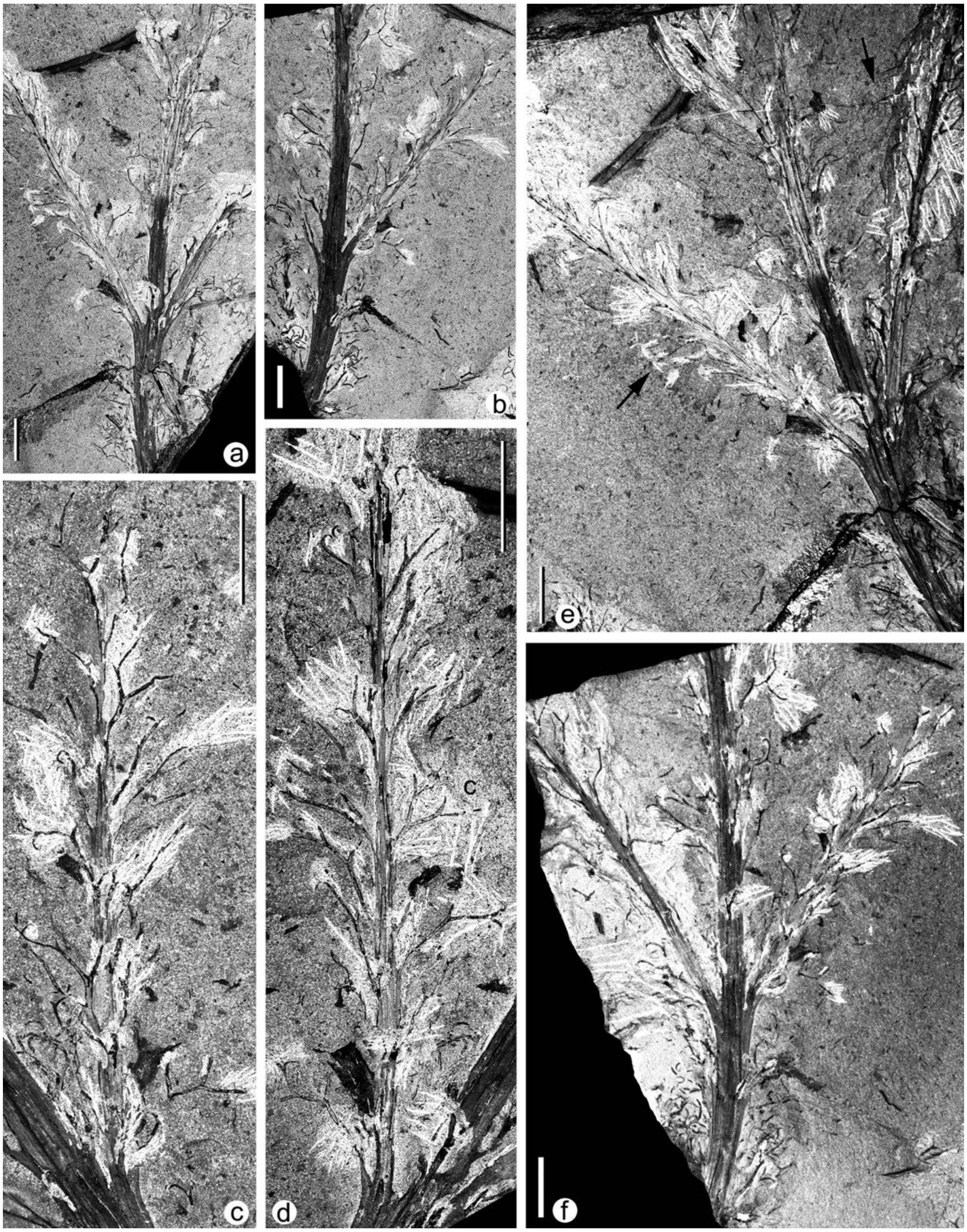

Fig. 5 *Compsocradus givetianus* (Wang DM) Fu, Wang Y, Berry et Xu comb. nov. from Xinjiang. *a*, *b*, *e*, *f*, Part and counterpart of first-order axis with second-order axis (arrow in *e*) and appendages. Specimen PB 20323a&b. *a*, *b*, Before dégagement. *e*, *f*, After dégagement (see fig. 6). *c*, *d*, Second-order axes with appendages indicated by arrows in *e*; *c* is right-hand branch and *d* is left-hand branch in *e*. Scale bars = 10 mm.

Basionym. *Ramophyton givetianum* Wang 2008, p. 1101; figures 2–5, 6*a*–6*e*, 8–13. Not figures 6*f*, 6*g*, 7. Also illustrated as *Barrandeina dusliana* (Krejči) Stur. Dou et al. (1983), p. 580; plate 205, figure 6; plate 206, figures 4, 5.

Holotype. XZH25a&b (Wang 2008, his fig. 3*a*, 3*b*).

Paratypes. XZH05a&b, XZH06a&b, XZH09a&b, XZH10a&b, XZH13a, XZH21a&b, XZH26a&b (Wang 2008).

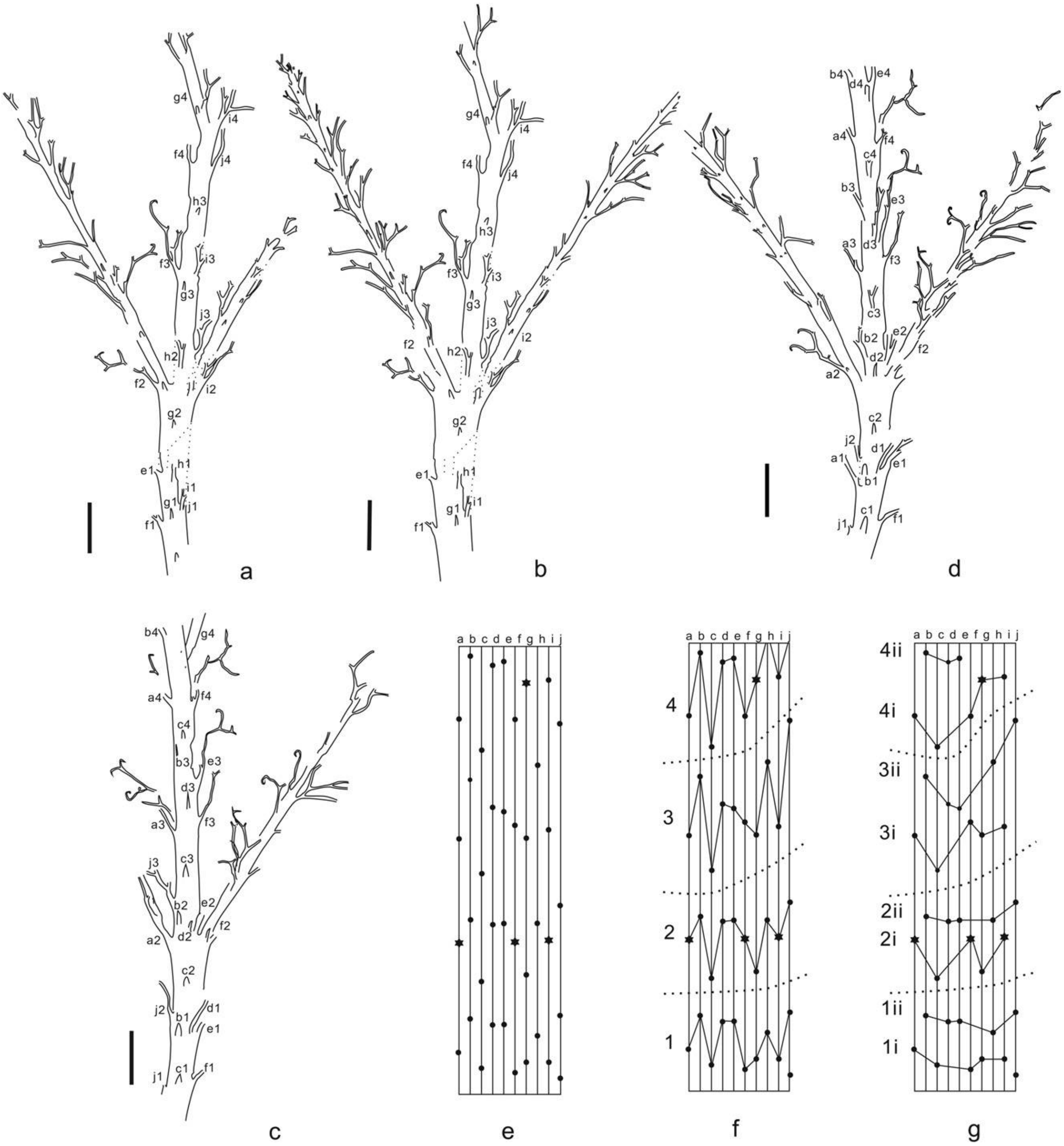

Fig. 6 *Compsocradus givetianus* (Wang DM) Fu, Wang Y, Berry et Xu comb. nov. from Xinjiang. Line drawing showing dégagement of the first-order axis, part and counterpart, specimen PB 20323a&b. *a*, Part before dégagement. *b*, Part after dégagement (see fig. 5*a*, 5*e*). *c*, Counterpart before dégagement. *d*, Counterpart after dégagement (see fig. 5*b*, 5*f*). *e*–*g*, Diagrammatic representation of the insertion of appendages and branches spread around the complete axis. *Circles* = appendages; *stars* = second-order branches. *e*, All bases. *f*, Bases divided into four cycles (1–4). *g*, Cycles divided into two loose whorls (i, ii). Scale bars = 10 mm.

New figured material. PB 20322a&b (figs. 2–4, 12, 13), PB 20323a&b (figs. 5, 6), PB 20324a&b (figs. 7, 8, 11), PB 20325a&b (figs. 9, 10), PB 20326 (figs. 14*a*, 14*d*, 15*b*), PB 20327 (figs. 14*b*, 15*a*), PB 20328 (figs. 14*c*, 15*c*), PB 20329 (fig. 14*e*), PB 20330 (fig. 14*f*).

Locality. South slope of small hill (251 Hill), ~20 km north of Hoxtolgay town, Hobuksar Menggol Autonomous County, North Xinjiang, China.

Stratigraphic horizon. Hujiersite Formation, Middle Devonian.

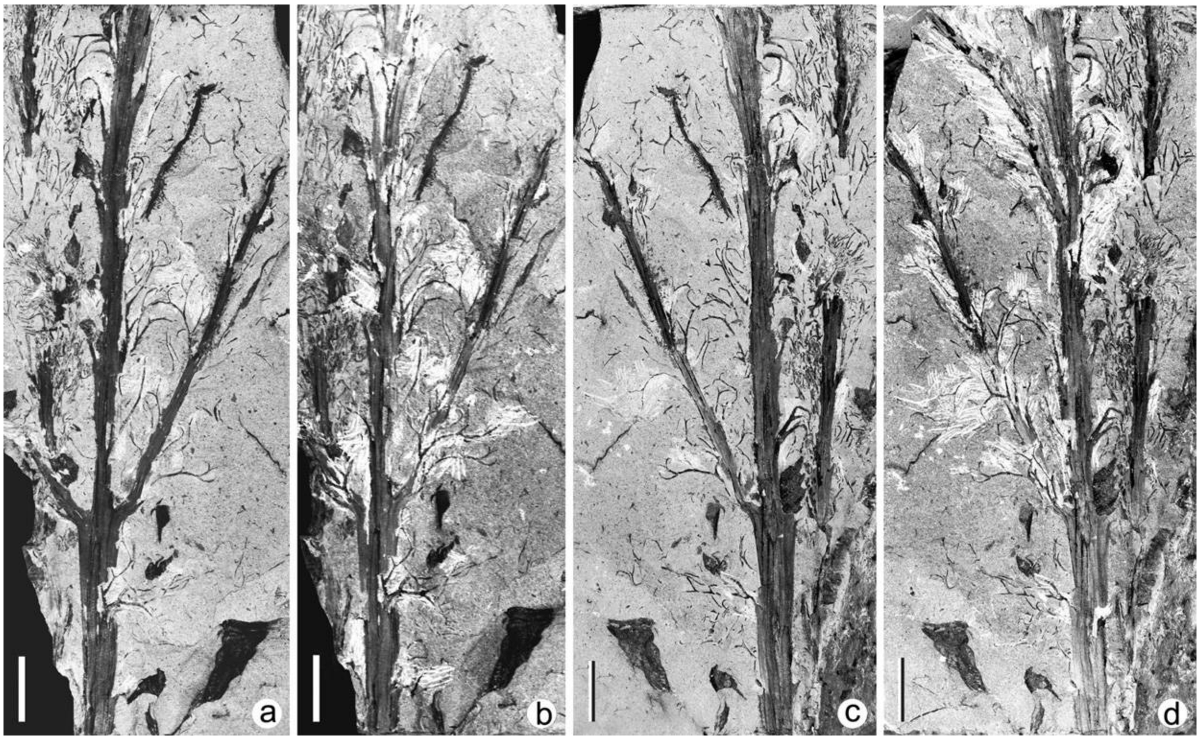

Fig. 7 *Compsocradus givetianus* (Wang DM) Fu, Wang Y, Berry et Xu comb. nov. from Xinjiang. *a*, *c*, Part and counterpart of first-order axis with second-order axes and appendages, before dégagement. Specimen PB 20324a&b. *b*, *d*, After dégagement. Scale bars = 10 mm.

Emended diagnosis. Plants as generic diagnosis. First-order axes 3.0–6.0 mm in diameter ($\overline{X} = 4.8$ mm, $n = 13$), up to at least 260 mm long; second-order axes 1.8–3.0 mm in diameter ($\overline{X} = 2.5$ mm, $n = 35$), up to at least 80 mm long; third-order axes 0.8–1.5 mm in diameter, ~20 mm long. Laterals (higher-order axes or appendages) attached in vertical ranks to parent axis, 10 on the first order, six or more on the second order, and at least four along the third order. Ultimate appendages inserted predominantly acutely, up to 0.7 mm diameter at base and up to 8–10 mm long, branching isodichotomously up to five times, either sterile or partially or wholly sterile; sterile tips and fertile tips recurved, the fertile bearing paired terminal sporangia. Sporangia fusiform in outline, 0.6–1.2 mm long and 0.2–0.6 mm wide.

Comments. The specimens show only morphological features; the anatomical structure of the plant is not preserved. Our measurements concentrated on specimens that have three orders of branching in organic connection. The measurements of axes presented by Wang (2008) probably represent a number of axes equivalent to our first-, second-, and third-order axes. Wang (2008) gives the length of appendages as up to 20.0 mm long yet provided no supporting description or illustration. He also gave distances between nodes as parts of the specific diagnosis, but because the nodes are so variable in their individual longitudinal extent, we omit them.

The specimens figured by Wang (2008, his figs. 6*f*, 6*g*, 7), showing densely recurved tips, are excluded, since our collections and the observations in Wang's material demonstrate the presence of another plant at this locality that is not *Compsocradus* (Fu 2006), to which this type of axis belongs.

Description

The description is based on ~120 specimens from 80 slabs. Three orders of axes are observed in connection (figs. 2*b*, 3*b*). Isodichotomously divided sterile and fertile appendages are attached to all three orders of branching. Both higher-order axes and appendages are inserted in vertical ranks along their parent axis, and we show that they are arranged in cycles, subdivided into loose whorls. In a loose whorl, laterals are inserted in about half of the ranks, and in the next loose whorl, the other ranks have laterals attached.

First-Order Axes

The first-order axes are 3.0–6.0 mm in diameter (figs. 2*a*, 2*b*, 3, 5*a*, 5*b*, 5*e*, 5*f*, 6*a*–6*d*, 7, 8*a*–8*d*, 9*a*–9*d*, 10*a*–10*d*) and are straight (figs. 5*a*, 5*b*, 5*e*, 5*f*, 6*a*–6*d*) or gently curved (figs. 2*a*, 2*b*, 9*a*–9*d*) with a smooth surface. The longest specimen is 260 mm long, and both ends are broken. On the basis of the overall radial symmetry of the branching system, this may represent the upright stem of the plant, but it remains possible that a larger order of axis might exist.

The first-order axes bear numerous overlapping appendages and second-order axes (figs. 2*a*, 2*b*, 3, 5*a*, 5*b*, 5*e*, 5*f*, 6*a*, 6*d*, 7, 8*a*–8*d*, 9*a*–9*d*, 10*a*–10*d*). The bases of both organs are marked by inverted V- or U-shaped depressions (fig. 2*a*, 2*d*), and the proximal margins of those depressions continue longitudinally down the stem for a distance of ~8–10 mm. These longitudinal lines allow the longitudinal ranks in which the laterals are inserted to be established.

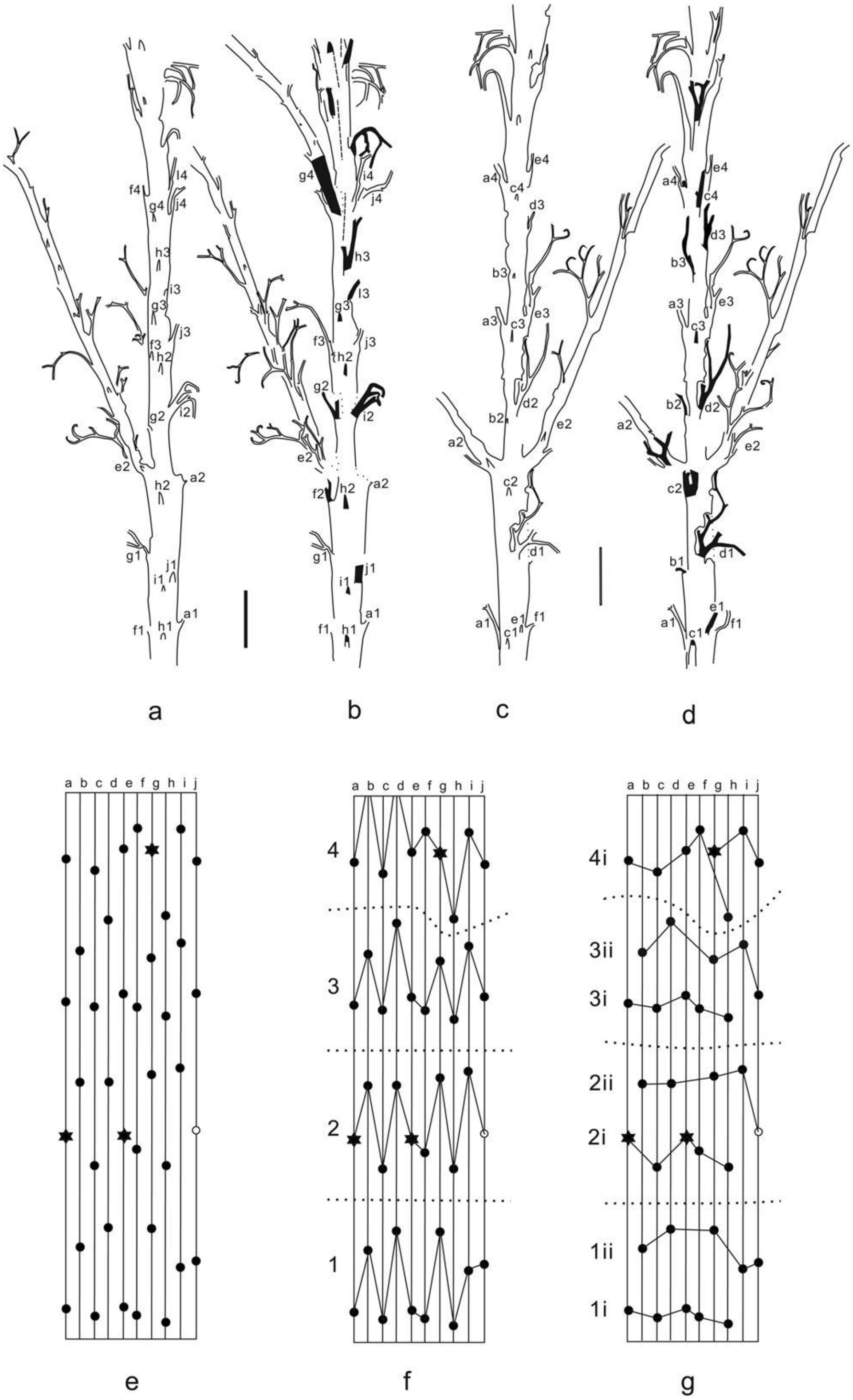

Fig. 8 *Compsocradus givetianus* (Wang DM) Fu, Wang Y, Berry et Xu comb. nov. from Xinjiang. Line drawings showing the dégagement of the first-order axis, part and counterpart. Specimen PB 20324a&b. *a*, Part before dégagement (see fig. 7*a*). *b*, Part after dégagement (see fig. 7*b*). *c*, Counterpart before dégagement (see fig. 7*c*). *d*, Counterpart after dégagement (see fig. 7*d*). Black appendages are going down into the matrix. *e*–*g*, Diagrammatic representation of the insertion of appendages and branches spread around the complete axis. Solid circles = appendages; stars = second-order branches; open circles = uncertain. *e*, All bases. *f*, Bases divided into four cycles. *g*, Cycles divided into two loose whorls. Scale bars = 10 mm.

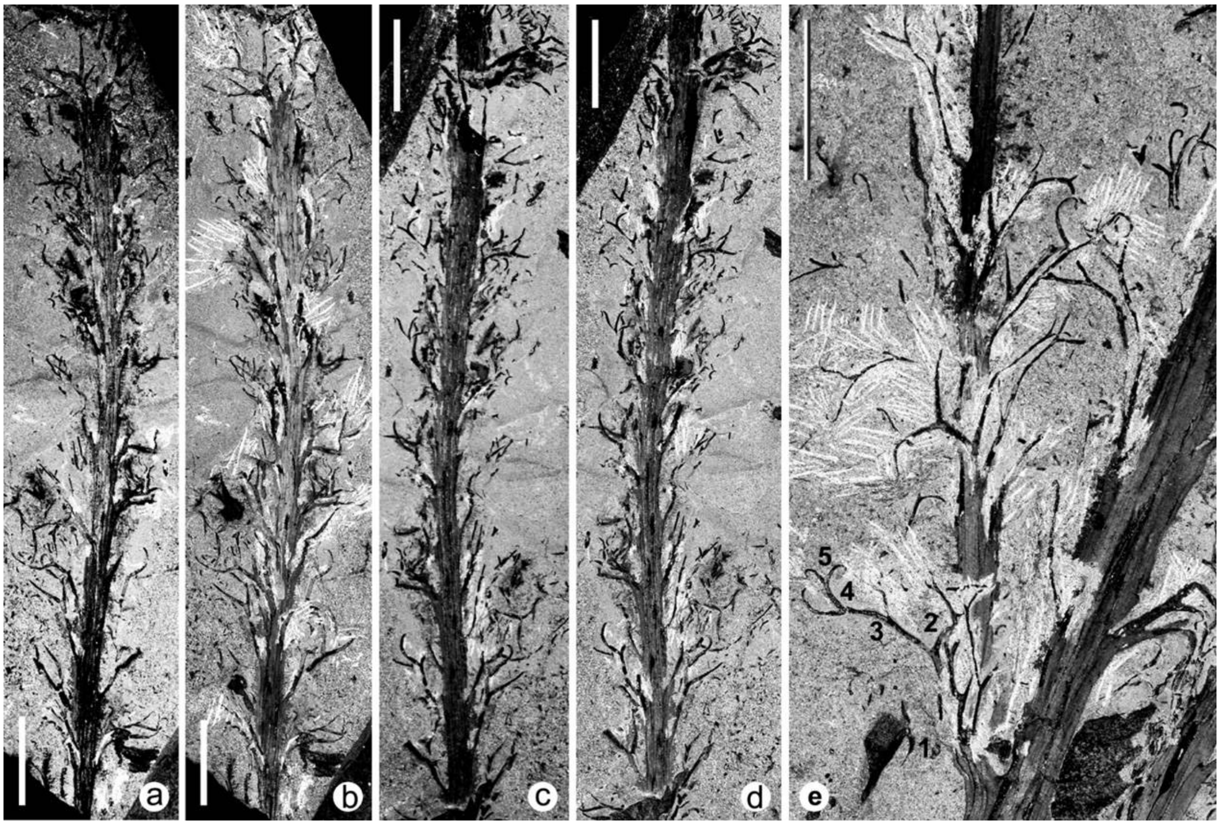

Fig. 9 *Compsocradus givetianus* (Wang DM) Fu, Wang Y, Berry et Xu comb. nov. from Xinjiang. *a*, *c*, Part and counterpart first-order axis with the second-order axes and appendages, before dégagement, specimen PB 20325a&b. *b*, *d*. After dégagement. *e*, Second-order axis with appendages, isodichotomously divided up to five times (numbered 1–5; from fig. 7*b*, left). Scale bars = 10 mm.

Second-Order Axes

Second-order axes, 1.5–3.0 mm in diameter, are inserted on the first-order axis at an angle of ~20°–45° (figs. 2*a*–2*e*, 3, 5*a*, 5*b*, 5*e*, 5*f*, 6*a*–6*d*, 7, 8*a*–8*d*, 9*a*–9*d*, 10*a*–10*d*, 11*a*–11*d*, 12*a*, 12*b*). The longest specimen is at least 100 mm long; however, one complete attached branch is only 80 mm long (fig. 5*e*, left arrow). Attached to second-order axes are both third-order axes and appendages in a three-dimensional manner.

Third-Order Axes

The third-order axes are 0.8–1.5 mm in diameter and at least 14 mm long (fig. 2*c*, 2*f*). Only appendages are attached on this order (figs. 2*f*, 13*a*).

Sterile Appendages

Sterile appendages are inserted on first- to third-order axes and are isodichotomously divided up to five times (figs. 5, 7, 8*a*–8*d*, 9*e* [dichotomies numbered 1–5], 11*a*–11*d*), with recurved tips (fig. 9*e*). Successive dichotomies are not in the same plane, and the overall pattern of branching is three-dimensional.

Fertile Appendages and Sporangia

Fertile appendages are borne on both the first- and the second-order axes (figs. 14*a*–14*e*, 15*b*). Fertile appendages consist of a supporting branching system and the sporangia. The branching systems have up to five isodichotomies (fig. 14*d*, numbered 1–5). The fertile appendages are up to 8–10 mm in maximum length (figs. 14*a*–14*e*, 15*a*, 15*b*), and each recurved tip terminates in a pair of sporangia (figs. 14*d*, 14*e*, 15*c*). Sporangia are fusiform in outline (fig. 14*f*), 1.0–1.2 mm long and 0.3–0.5 mm wide at the widest point (near to the middle), with an obtuse-cuspate apex. Epidermal cell outlines are visible on the coalified tissues of the surface of sporangia (fig. 14*f*). No obvious dehiscence structures can be seen in our specimens, but longitudinal dehiscence has been demonstrated by Wang (2008, p. 1107). SEM examination and HF maceration failed to show spores in situ.

Arrangement of Lateral Organs on First-Order Axes

First-order axes bear numerous appendages and second-order axes. In order to establish their insertion pattern, the specimens were almost completely destroyed by systematic dégagement, which was recorded by photographs and by line drawing.

Specimen PB 20322a&b (part and counterpart: fig. 2*a*, 2*b*; close-up: fig. 2*d*, 2*e*) are preserved over more than 100 mm.

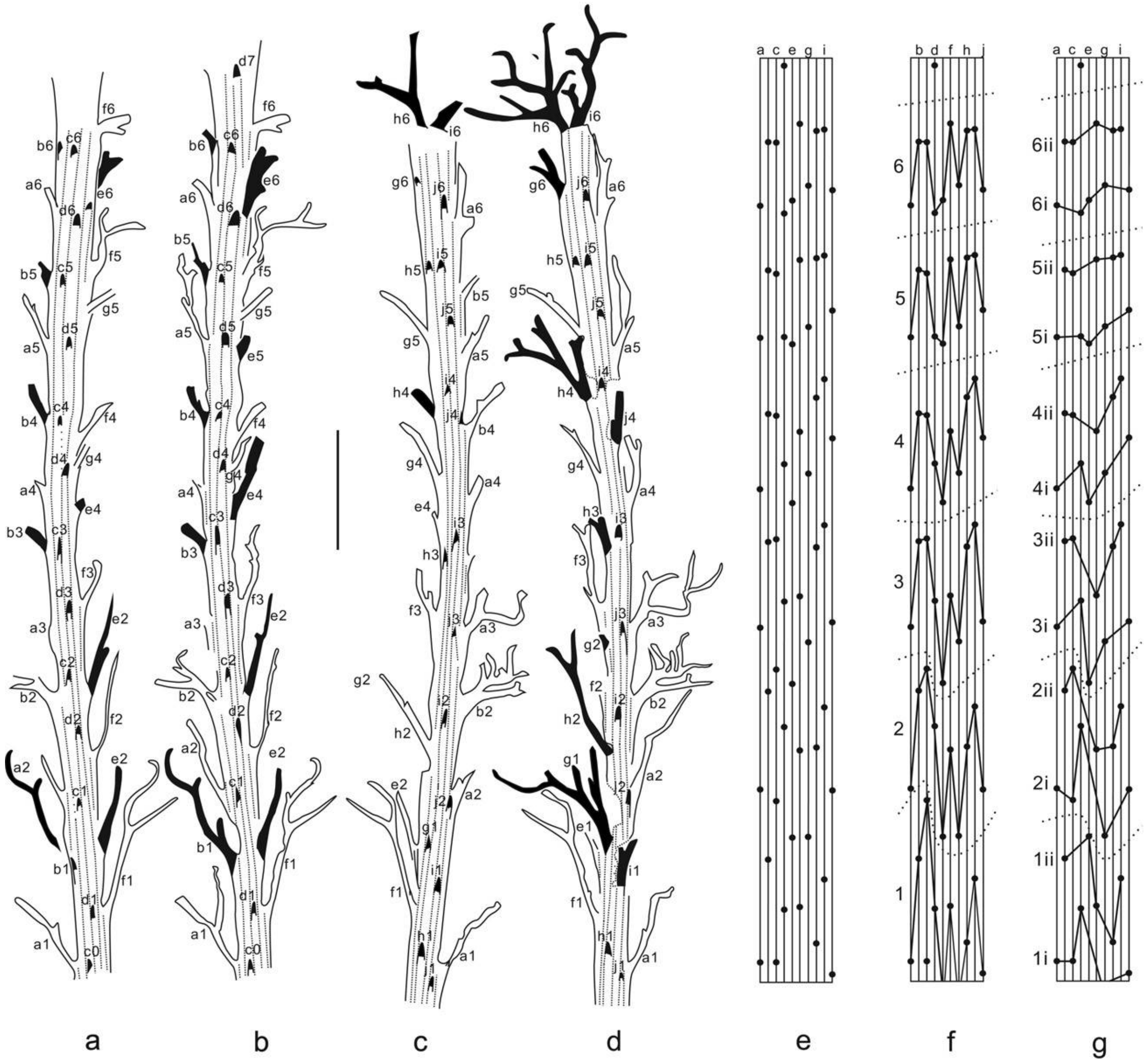

Fig. 10 *Compsocradus givetianus* (Wang DM) Fu, Wang Y, Berry et Xu comb. nov. from Xinjiang. Line drawing showing dégagement of first-order axis, part and counterpart. Specimen PB 20325a&b. *a*, Part before dégagement (see fig. 9*c*). *b*, Part after dégagement (see fig. 9*d*). *c*, Counterpart before dégagement (see fig. 9*a*). *d*, Counterpart after dégagement (see fig. 9*b*). *e–g*, Diagrammatic representation of the insertion of appendages and branches spread around the complete axis. Circles = appendages. *e*, All bases. *f*, Bases divided into six cycles (1–6). *g*, Cycles divided into two loose whorls (i, ii). Scale bars = 10 mm.

Line drawings of part (fig. 3*a*) and counterpart (fig. 3*b*) before and after initial dégagement show an apparently haphazard arrangement of insertion of laterals, but with careful scrutiny some repetitive patterns can be picked out. Second-order axes and appendages are attached to the first-order axis in 10 vertical ranks defined by longitudinal striations, and only three to five insertion points were clearly found for each rank from the lower area of the part and the counterpart (fig. 4*a*, 4*b*). The average longitudinal distance between neighboring insertion points in a rank ranges between 8 and 10 mm. The position of the insertion points has been mapped onto a diagram showing the full round of the axis surface (fig. 4*c*). Circles and stars representing appendages and second-order axes, respectively, are plotted at the level of the axil of the departing organ.

The attachments of second-order axes (fig. 4*c*, stars) cluster at two levels, with two and three inserted at each level. Furthermore, at the distal level, the positions of attachment are not repeated but occur in ranks that did not have second-order axes at the proximal level.

The insertion pattern of all lateral organs in the lower part of the axis was established (figs. 2*d*, 2*e*, 4). In rank *a* on the part and counterpart, one second-order branch and two appendage bases are observed (*a2*–*a4*). The second-order

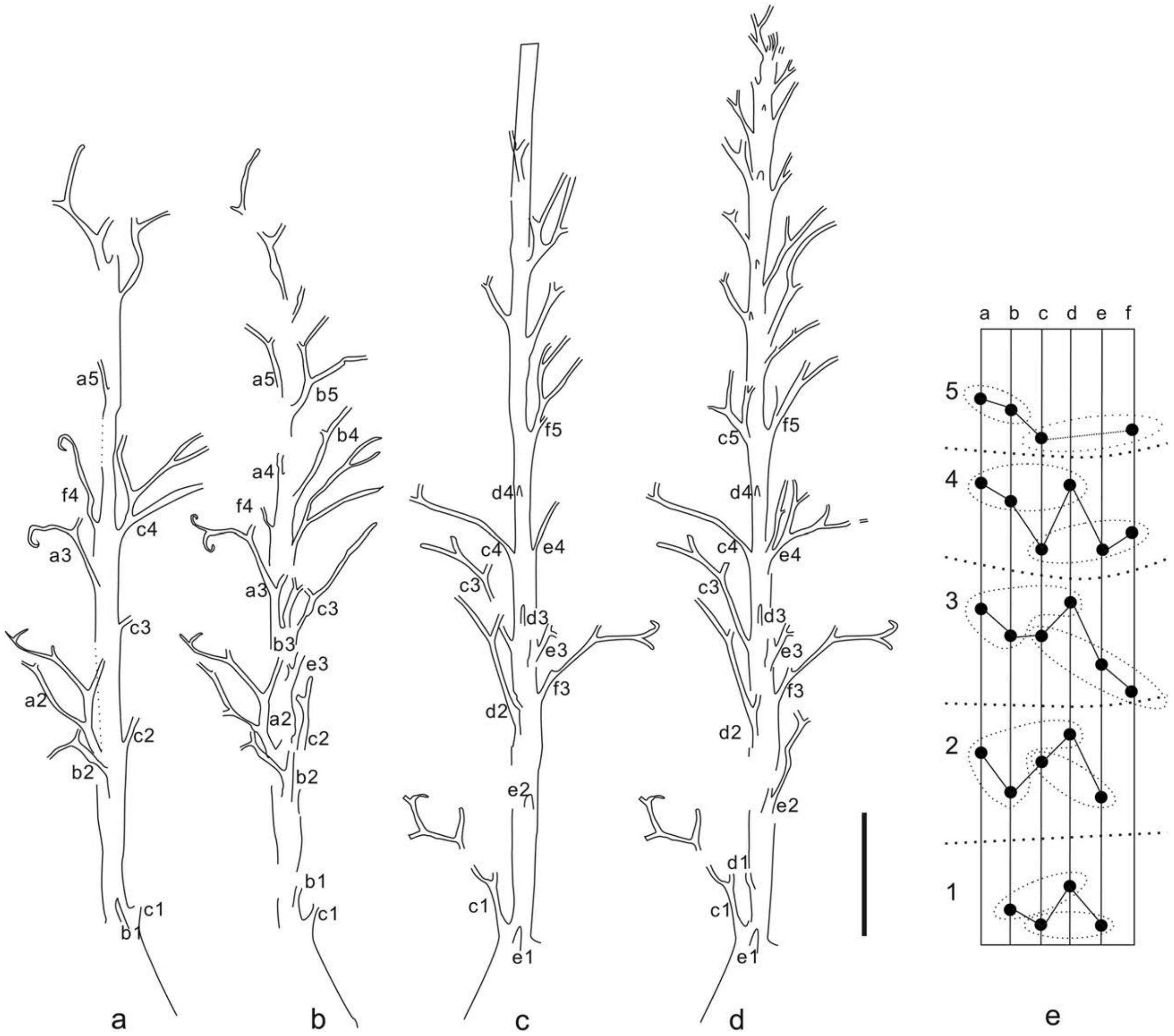

Fig. 11 *Compsocradus givetianus* (Wang DM) Fu, Wang Y, Berry et Xu comb. nov. from Xinjiang. Line drawing showing dégagement of second-order axis with part and counterpart. Specimen PB 20324a&b. *a*, Part before dégagement (see fig. 5*b*). *b*, Part after dégagement (see fig. 5*c*). *c*, Counterpart before dégagement (see fig. 5*a*). *d*, Counterpart after dégagement (see fig. 5*d*). *e*, Diagrammatic representation of the insertion of appendages, divided into five cycles (1–5), each cycle divided into two loose whorls (dotted lines). Circles = appendages. Scale bar = 10 mm.

branch (*a2*) is connected with the first-order axis only on the counterpart. In rank *b* on the part, two appendage bases (*b2*, *b3*) and one second-order branch are observed (*b4*). Second-order branch *b4* was exposed by dégagement. In ranks *c*, *d*, and *e* on the part, four, three, and three appendages are observed, respectively, and are visible only as inverted U-shaped depressions, all departing downward in the middle of the axis. The laterals are identified as appendages rather than axes on the basis of their size. In rank *f* on the part and counterpart, one second-order branch (*f1*) and three appendages are observed. In rank *g* on the counterpart, three appendages and one second-order axis (*g4*) are observed. Those visible on the margin of the counterpart axis go down into the matrix below the level of branch *f1* (fig. 2*b*). In ranks *h*, *i*, and *j* on the counterpart, attachments of three, four, and three laterals are observed; *i4* is a second-order branch.

Overall, the second-order axes and appendages are inserted in a repeating pattern, which involves all 10 ranks in each cycle (for definition, see "Material and Methods"). Cycles numbered 1–4 are indicated in figure 4*d*. Each cycle can be broken down visually into two subcycles or loose whorls (fig. 4*e*). The proximal of the loose whorls in each cycle (*i*) has a pattern, with one or two adjoining ranks having laterals followed around the stem by one or two ranks that do not have laterals. In the distal of the loose whorls in each cycle (*ii*), the pattern is reversed, with those ranks previously having laterals not having laterals and those previously having them not having them.

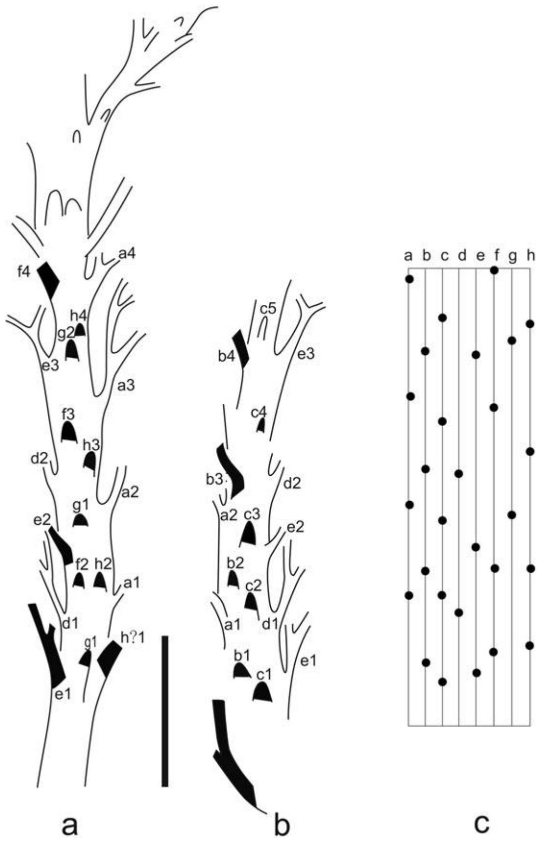

Fig. 12 *Compsocradus givetianus* (Wang DM) Fu, Wang Y, Berry et Xu comb. nov. from Xinjiang. Line drawing of dégagement of the second-order axis from specimen PB 20322a&b. *a*, Part after dégagement (see fig. 2*b*). *b*, Counterpart after dégagement (see fig. 2*a*). *c*, Diagrammatic representation of the insertion of appendages. Circles = appendages. Scale bar = 10 mm.

The same pattern is observed from three other specimens (figs. 6, 8, 10). Each has 10 vertical ranks, and similar cycles and loose whorls can be interpreted from the insertion patterns. In specimen PB 20323 (figs. 5*a*, 5*b*, 5*e*, 5*f*, 6), the cycles and loose whorls are very clear proximally but become obliquely intercalated distally. Second-order branches are clustered at the level of cycle 2. In specimen PB 20324 (figs. 7, 8), the patterns of cycles seem very clear, but the pattern of loose whorls within them is less consistent. In specimen PB 20325a&b (figs. 9, 10), the pattern of cycles and loose whorls is very clear distally, but proximally they are obliquely intercalated. Therefore, from specimen to specimen, the exact arrangement of laterals on compressions is not the same.

Arrangement of Third-Order Axes and Appendages on Second-Order Axes

The pattern of third-order branches and appendages along the second-order axes was best demonstrated by specimens PB 20322 and PB 20323, where the second-order axis is attached to the first-order axis and part and counterpart were available for study. In specimen PB 20323 (figs. 5*c*, 5*d*, 11), the second-order axis is preserved over a length of 80 mm, and appendages are attached in six ranks. The average distance between neighboring insertion points in the same rank ranges from 5 to 7 mm. The horizontal pattern is not very clear (fig. 11*e*). Cycles of six inserted laterals are clearly distinct. A division of each cycle into two loose whorls is not as obvious as in the first-order axis.

In specimen PB 20322 (figs. 2*c*, 12), the pattern appears more complex than that in PB 20323a&b (fig. 5*a*, 5*b*). First, there are some problems in delimiting the ranks. There may be a reduction in the number of ranks (and therefore primary xylem ribs) along the axis. Second, the axis is very small and may have been more distorted during preservation. Nevertheless, some regular patterning is observed, for example, the regular alternation of rank with ranks *a*, *b* and *b*, *c*.

Arrangement of Appendages on Third-Order Axes

The third-order axis is preserved for only 14 mm, and four vertical ranks of appendages are attached without counterpart (figs. 2*f*, 13*a*, 13*b*). It is possible that about six vertical ranks of appendages should be arranged on the third-order axis. No pattern can be determined precisely.

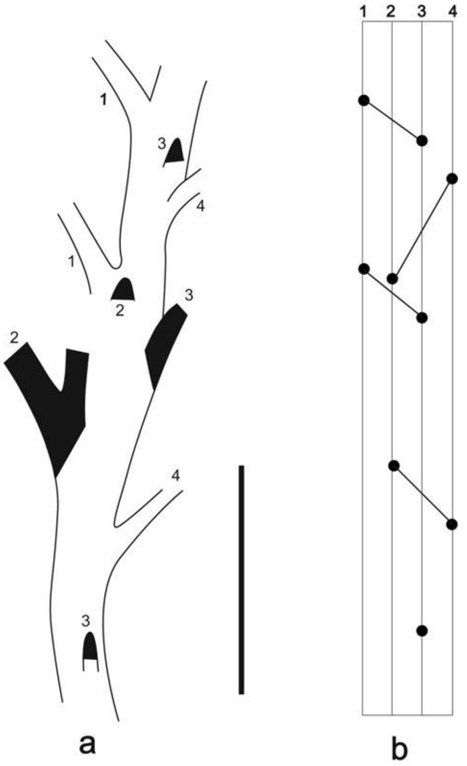

Fig. 13 *Compsocradus givetianus* (Wang DM) Fu, Wang Y, Berry et Xu comb. nov. from Xinjiang. Line drawing of dégagement of third-order axis from specimen PB 20322a&b. *a*, Part after dégagement (see fig. 2*f*). *b*, Diagrammatic representation of the insertion of appendages. Circles = appendages. Scale bar = 10 mm.

Fig. 14 *Compsocradus givetianus* (Wang DM) Fu, Wang Y, Berry et Xu comb. nov. from Xinjiang. *a–c*, *e*, Fertile appendages attached to the first- and second-order axes, consisting of the supporting branching system and paired sporangia at the recurved tip. *a*, *c*, Specimen PB 20326, 20328. *b*, *e*, Specimen PB 20327, 20329. Scale bars = 10 mm. *d*, Supporting branching system with up to five isodichotomies (numbered 1–5), with terminal recurved paired sporangia, after partial dégagement in *a*. Scale bar = 10 mm. *f*, Paired sporangia. Specimen PB 20330. Scale bar = 1 mm.

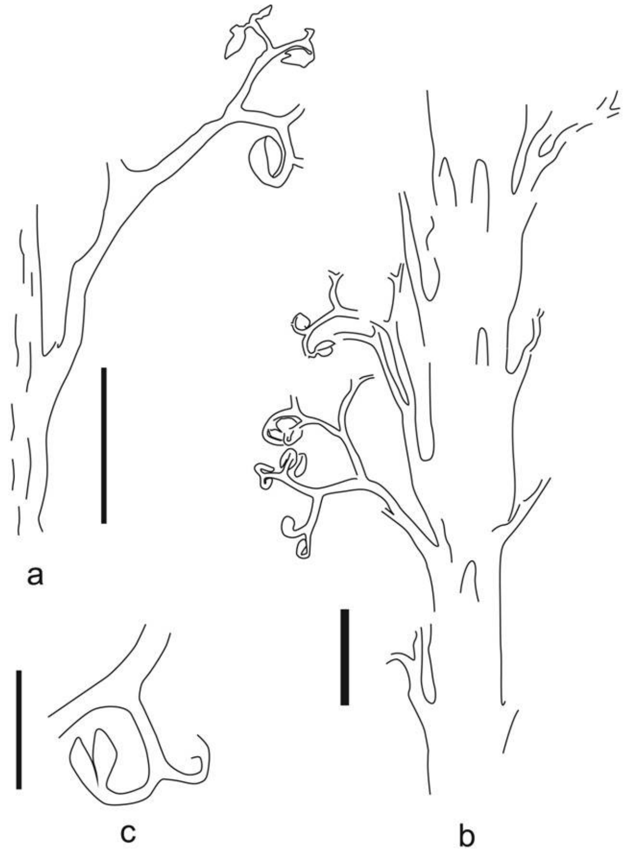

Fig. 15 *Compsocradus givetianus* (Wang DM) Fu, Wang Y, Berry et Xu comb. nov. from Xinjiang. Line drawing of the fertile appendages and sporangia. *a*, Fertile unit (see fig. 14*b*). *b*, Branch with fertile units (see fig. 14*d*). *c*, Terminal paired sporangia (see fig. 14*c*). Scale bars = 10 mm.

Compsocradus laevigatus *Berry et Stein (Figs. 16, 17)*

The branching patterns in *Compsocradus laevigatus*, the type species, was evaluated by Berry and Stein (2000) on the basis of anatomy and some compression specimens, which showed six ranks of laterals. The pattern described was for whorls in which laterals were emitted from every other rib of the stele; in alternate whorls, the ribs from which the laterals were emitted—and therefore their positions on the axis surface—were offset. However, one specimen, NMW 93.97G.35 (see Berry and Stein 2000, their figs. 3*a*, 3*b*, 6), showed four laterals in the basal whorl which was pointed out as an anomaly.

On the basis of our new understanding of more complex branching patterns in *Compsocradus givetianus*, we reexamined this Venezuelan specimen to see whether complete cycles of more then six laterals were present. Following our dégagement of the specimen, two additional appendages (*e*2, *g*3) were revealed (figs. 16*b* [arrows], 17*a*–17*e*). This axis therefore has seven ranks of appendages along the preserved length. From bottom to top, the number of appendages for each loose whorl changes from four to three to four to three to four (fig. 17*e*). Note that this means that in some loose whorls (1ii, 2ii, 3ii), two neighboring ranks (*a* and *g*) emit laterals, just as interpreted on a more extensive basis in *C. givetianus*. For comparison, appendage insertion diagrams for six-ranked specimens NMW 93.97G.34 (Berry and Stein 2000, their figs. 1, 2) and NMW 93.97G.36 (Berry and Stein 2000, their figs. 2*e*, 2*f*, 4) were also prepared (fig. 17*f*, 17*g*). These new diagrams show longitudinal as well as rank spacing to allow direct comparison with our similar diagrams for the new species. The new data presented for *C. laevigatus* from Venezuela (fig. 17*d*–17*g*) show that the insertion patterns are almost as variable as those in *Compsocradus recurvatus*, but can perhaps be more easily visually separated into loose whorls and internodes.

Identity and Comparisons

Identity at Genus Level

In the descriptions above, we have expanded and clarified the diversity and variability of branching patterns in *Compsocradus laevigatus*, the type species from Venezuela. We have also enlarged the concept and clarified the understanding of branching patterns for the recently described plant from Xinjiang, now attributed to *Compsocradus givetianus*.

In the type species, the established branching pattern was until now based on a six-ribbed stele. We have expanded that understanding to a compression specimen with seven apparent ranks of laterals. In that specimen, we have recognized the presence of laterals in adjacent ranks in the same

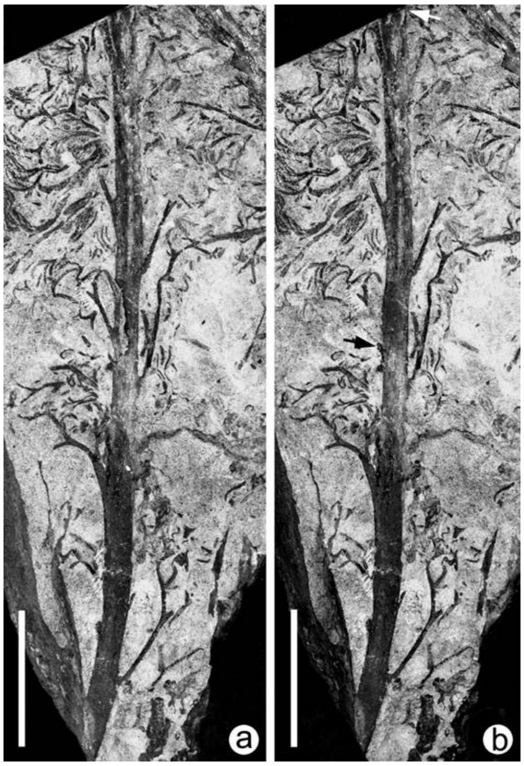

Fig. 16 *Compsocradus laevigatus* Berry et Stein 2000 from Venezuela. First-order axis, specimen NMW93.97G.35b. *a*, Before further dégagement. *b*, After dégagement (also see Berry and Stein 2000, their fig. 3*b*). Arrows indicate newly uncovered appendages. Scale bars = 20 mm.

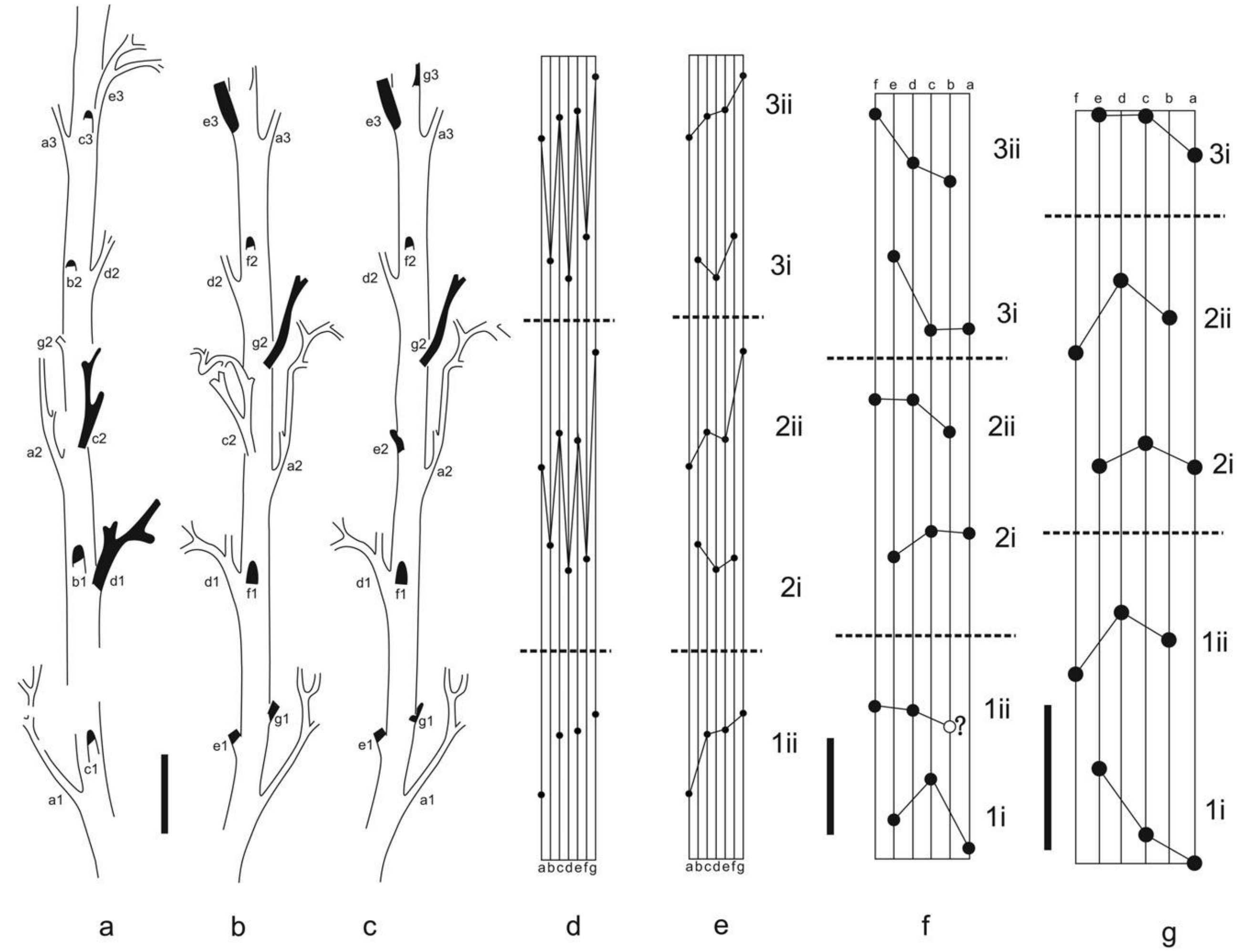

Fig. 17 *Compsocradus laevigatus* Berry et Stein 2000 from Venezuela. Line drawing of the first-order axes as figured by Berry and Stein (2000). *a*, *b*, Part and counterpart showing seven apparent ranks. Specimen NMW93.97G.35a&b (Berry and Stein 2000, their figs. 3*b*, 6*b*). Black appendages are those that go downward into the matrix. *c*, After our further dégagement of *b*, showing the newly exposed appendage *e2*. *d*, *e*, Diagrammatic representation of the insertion of appendages (circles), showing overall pattern of cycles 1–3 (*d*) and loose whorls identified from proximal and distal levels within cycles. *f*, *g*, Diagramatic representation of the insertion of appendages in further specimens with six apparent ranks. *f*, From specimen NMW93.97G.34a&b (Berry and Stein 2000, their figs. 1, 2). *g*, From specimen NMW93.97.36a&b (Berry and Stein 2000, their figs. 3*e*, 3*f*, 4). Circles = appendages. Scale bars = 10 mm.

loose whorl. Furthermore, it is clear that the organization of the loose whorls, when plotted correctly in longitudinal position in all specimens (fig. 17*e*–17*g*), is not as obvious as was perhaps implied in the original description and diagrams of Berry and Stein (2000).

Branching patterns in the widest axes of *C. givetianus* from Xinjiang are shown in this article to be very similar to those now recognized for the type species, excepting that there are more ranks (up to 10) and that the cycles and loose whorls are less clearly separated longitudinally. Specifically, the position of laterals from adjacent ranks tends to allow them to be separated into two groups at a proximal and distal level here termed loose whorls. However, our understanding of the mode of development of this pattern or its significance is woefully limited.

Although the generalities of axis and appendage morphology and branching patterns are extremely similar, excepting the presumed number of xylem ribs, there is one consistent difference that allows the plants to be placed in different species. The sporangia of the Xinjiang specimens are consistently recurved.

Comparison to Rotoxylon dawsonii *(Dawson) Cordi et Stein*

The type specimen of *Rotoxylon dawsonii* (Dawson 1882) has most recently been classified as an iridopteridalean stem (Cordi and Stein 2005). It has a diameter of at least 15 mm, with 18 primary xylem ribs. The authors considered that the vascular system was originally dissected, but we consider there is a possibility that this dissection is taphonomic, caused by compaction of a brittle, deeply lobed, xylem column. For the purposes of comparison with *C. givetianus*, the pattern of trace departures is most important. Traces are seen to be in orthostichies but regularly offset between successive whorls.

This regular offset is achieved in two ways. First, there are in some cases regular alternations in the symmetry of successive trace departures, which occur not in the midplane of the xylem rib but to one side and then the other. Second, there is evidence that alternate or near alternate ribs produce traces in one whorl, and then the ribs that did not produce traces in the first whorl produce traces in the subsequent whorl. The first method of producing offset whorls is not seen in *C. laevigatus*, for which only limited numbers of trace departures have been observed. However, the second method was inferred. Furthermore, the details relating to *R. dawsonii*, with trace departures sometimes being derived from two or more adjacent ribs in the alternating whorls, make the patterns observed very similar to the more complex patterns observed in *C. givetianus*.

It is therefore clear that although the full complexity of patterns of trace departure as observed in *Rotoxylon* have not been interpreted from morphologically preserved compression fossils, the patterns of trace departure we observe in *C. givetianus* are well within the variation of trace departure now known from the Iridopteridales. This includes both the alternating, regularly offset pattern of insertion of laterals and the close imbrication of whorls.

Comparison to Other Iridopteridalean and Cladoxylopsid Plants

A pairwise comparison of *Compsocradus* to other related Iridopteridalen plants was made by Berry and Stein (2000), and those comparisons are still largely valid. More recent discoveries of additional similar plants (e.g., *Denglongia hubeiensis* Xue et Hao [Xue and Hao 2008; Xue et al. 2009] from the Frasnian of South China) have also made their own comparisons, which also remain valid.

The most interesting question is how branching patterns in pseudosporochnalean plants might relate to *Compsocradus* and *Rotoxylon*. Stein and Hueber (1989) give the most detailed analysis of the production of vascular traces on a lateral branch attributed to *Pseudosporochnus hueberii*, which is said to be three-dimensional but neither helical nor whorled. It is immediately apparent that with the higher number of xylem ribs (20–50) and multiple traces entering appendages from adjacent ribs, the patterns are even harder to establish than in our plant, and the only comparisons we could make at this stage would be superficial.

Conclusions

The plant described here, *Compsocradus givetianus*, the distal parts of which were previously assigned to *Rhamophyton givetianum* (Wang 2008), is here shown to be characterized by a branching pattern that appears both loosely whorled and regularly offset. We have no knowledge of the anatomy and in situ spores. On morphological characters, this plant is placed in the genus *Compsocradus* on the basis of the original description of the type species, *Compsocradus laevigatus* from Venezuela by Berry and Stein (2000), and on new observation of that original material. Berry and Stein (2000) classified *C. laevigatus* in the Iridopteridales of Stein (1982) on the basis of the close anatomical resemblance to the genus *Arachnoxylon kopfii* Read. *C. givetianus* from Xinjiang is a distinct species because of the small morphological differences in the number of observed vertical ranks and the recurved sporangia.

Of greatest interest, perhaps, is to understand exactly what was going on at the apex of the axes of *Compsocradus* and perhaps *Rotoxylon*. The observed patterns of insertion of laterals suggest alternating "pulsing" of formation of lateral meristems. In order to completely understand this, we would require extensively permineralized material in which we could be confident that there was no undue distortion of the specimen and preferably preserved apices themselves. Nonetheless, our understanding of the fundamental architectural parameters within the Iridopteridales is considerably increased by the discovery of this species. Perhaps the outcome of this behavior is to produce laterals that are more or less regularly offset, perhaps increasing photosynthetic potential.

In this study of the assemblages of the Hujiersite Formation, we are trying to determine the similarity or otherwise of the north Xinjiang flora to contemporary floras worldwide, on the basis of extensive collecting and detailed monographic description. *Compsocradus* is a genus only previously recognized from Venezuela. We will comment further on the paleogeographic significance of *Compsocradus* as the project progresses.

Acknowledgments

We thank Professors C. Y. Cai and Y. W. Dou for fieldwork support and valuable suggestions and D. M. Wang for access to his material. This research was supported by the Chinese Academy of Sciences for Y. Wang (KZCX2-YW-Q05-01); the National 973 Project for Y. Wang and H.-H. Xu (2006CB806400); the International Joint Project for C. M. Berry and Y. Wang between the National Natural Sciences Foundation of China (NFSC) and the Royal Society, London; and the NFSC (40902005). We thank an anonymous reviewer for comments that improved the manuscript and Dr. W. E. Stein, who provided many helpful and insightful suggestions to clarify the text.

Literature Cited

Arnold CA 1940 Structures and relationships of some Middle Devonian plants from western New York. Am J Bot 27:57–63.

Banks HP 1980 Floral assemblages in the Siluro-Devonian. Pages 1–24 *in* DL Dilcher, TN Taylor, eds. Biostratigraphy of fossil plants: successional and paleoecological analysis. Dowden, Hutchinson & Ross, Stroudsburg, PA.

Berry CM 2005 "*Hyenia*" *vogtii* Høeg from the Middle Devonian of Spitsbergen: its morphology and systematic position. Rev Palaeobot Palynol 135:109–116.

Berry CM, D Edwards 1996 *Anapaulia moodyi* gen. et sp. nov., a probable iridopteridalean compression fossil from the Devonian of Venezuela. Rev Palaeobot Palynol 93:127–145.

Berry CM, M Fairon-Demaret 2001 The Middle Devonian flora revisited. Pages 120–139 *in* PG Gensel, D Edwards, eds. Plants invade the land: evolutionary and environmental perspectives. Columbia University Press, New York.

Berry CM, WE Stein 2000 A new Iridopteridalean from the Devonian of Venezuela. Int J Plant Sci 161:807–827.

Cai CY 2000 Non-marine Devonian of China. Pages 103–123 *in* Nanjing Institute of Geology and Palaeontology, Chinese Academy of Sciences, eds. Stratigraphic correlation charts in China with explanatory text. Science, Beijing. (In Chinese.)

Cai CY, Wang Y 1995 Devonian floras. Pages 28–77 *in* X Li, ed. Fossil floras of China through the geological ages. Guangdong Science and Technology, Guangzhou.

Cordi J, WE Stein 2005 The anatomy of *Rotoxylon dawsonii* comb. nov. (*Cladoxylon dawsonii*) from the Upper Devonian of New York State. Int J Plant Sci 166:1029–1045.

Dawson JW 1881 Notes on new Erian (Devonian) plants. Q J Geol Soc Lond 37:299–308.

——— 1882 The fossil plants of the Erian (Devonian) and Upper Silurian formations of Canada. Can Geol Surv 2:126.

Dou YW, ZH Sun, SZ Wu, DY Gu 1983 Vegetable kingdom. Pages 561–614 *In* Geological Surveying Team and Institute of Geoscience, Xinjiang Bureau of Geology, Geological Surveying Department, Xinjiang Bureau of Petroleum, eds. Palaeontological atlas of northwest China, Xinjiang Uygur autonomous region. Vol 2. Geological Publishing House, Beijing. (In Chinese.)

Edwards D, M Fairon-Demaret, CM Berry 2000 Plant megafossils in Devonian stratigraphy: a progress report. Cour Forschungsinst Senckenb 220:25–37.

Fairon-Demaret M, J Hilton, CM Berry 1999 Surface preparation of macrofossils (dégagement). Pages 33–35 *in* TP Jones, NP Rowe, eds. Fossil plants and spores: modern techniques. Geological Society, London.

Fu Q 2006 Study on some non-lycopsids from the Hujiersite Formation (late Middle Devonian) of North Xinjiang, China. PhD diss. Graduate School of the Chinese Academy of Sciences.

Kenrick P, PR Crane 1997 The origin and early diversification of land plants: a cladistic study. Smithsonian Institution, Washington, DC. 437 pp.

Leclercq S 1960 Réfendage d'une roche fossilifière et dégagement de ses fossiles sous binoculaire. Senckenb Lethaea 41:483–487.

Liu SW 1990 Fossil conchostracaus of "Zhulumute Formation" in Tacheng, Xinjiang and their age. J Hebei College Geol 13:44–49. (In Chinese with English abstract.)

Lu LC 1997 Miospores from the Hujiersite Formation at Aherbruckomha in Hoboksar, Xinjiang. Acta Micropalaeontol Sin 14:295–314. (In Chinese with English abstract.)

Read CB 1938 Some Psilophytales from the Hamilton group in western New York. Bull Torrey Bot Club 65:599–606.

Skog JE, HP Banks 1973 *Ibyka amphikoma*, gen. et sp. n., a new protoarticulate precursor from the late Middle Devonian of New York State. Am J Bot 60:336–380.

Stein WE 1982 *Iridopteris eriensis* from the Middle Devonian of North America, with systematics of apparently related taxa. Bot Gaz 143:401–416.

——— 1993 Modeling the evolution of stellar architecture in vascular plants. Int J Plant Sci 154:229–263.

Stein WE, FM Hueber 1989 The anatomy of *Pseudosporochnus*: *P. hueberi* from the Devonian of New York. Rev Palaeobot Palynol 60:311–359.

Stein WE, DC Wight, CB Beck 1984 Possible alternatives for the origin of Sphenopsida. Syst Bot 9:102–118.

Wang DM 2008 A new iridopteridalean plant from the Middle Devonian of northwest China. Int J Plant Sci 169:1100–1115.

Wang DM, YJ Lin 2007 A new species of *Metacladophyton* from the Late Devonian of China. Int J Plant Sci 168:1067–1084.

Wang Y, HH Xu, Q Fu, P Tang 2004 A new diminutive plant from the Hujiersite Formation (late Middle Devonian) of North Xinjiang, China. Acta Palaeont Sin 43:461–471. (In Chinese with English abstract.)

Wang Z, B Geng 1997 A new Middle Devonian plant: *Metacladophyton tetrapetalum* gen. et sp. nov. Palaeontogr Abt B 243:85–102.

Wight DC 1987 Non-adaptive change in early land plant evolution. Palaeobiology 13:208–214.

Xiao SL, HF Hou, SZ Wu 1992 The researches of Devonian system in North Xinjiang. Xinjiang Science Technology and Hygiene, Urumqi. (In Chinese.)

Xu HH 2006 Study on some herbaceous lycopsids from the Hujiersete Formation, late Middle Devonian of North Xinjiang, China. PhD diss. Graduate School of the Chinese Academy of Sciences.

Xu HH, Y Wang, CM Berry, C-Y Cai 2008 Two species of *Haskinsia* Grierson et Banks (Lycopsida) from the Middle Devonian of Xinjiang, China, and consideration of their palaeogeographical significance. Bot J Linn Soc 157:633–644.

Xue JZ, SG Hao 2008 *Denglongia hubeiensis* gen. et sp. nov., a new plant attributed to Cladoxylopsida from the Upper Devonian (Frasnian) of South China. Int J Plant Sci 169:1314–1331.

Xue JZ, SG Hao, JF Basinger 2009 Anatomy of the Late Devonian *Denglongia hubeiensis*, with a discussion of the phylogeny of the Cladoxylopsida. Int J Plant Sci 171:107–120.